EUROPEAN ORGANIZATION FOR NUCLEAR RESEARCH

CERN/SPSC/P 73-1
27 July 1973

PROPOSAL TO STUDY HIGH-ENERGY NEUTRINO INTERACTIONS AT THE SPS

M. Holder, J. Steinberger, H. Wahl and E.G.H. Williams
CERN, Geneva, Switzerland

C. Geweniger*) and K. Kleinknecht
Institut für Physik, Dortmund

F. Eisele, V. Hepp, E. Kluge and K. Tittel*)
Institut für Hochenergiephysik, Heidelberg

M. Banner and R. Turlay
Centre d'Etudes Nuclaires de Saclay

*) Present address: CERN, Geneva, Switzerland.

1. INTRODUCTION

The only known feasible way to study the weak interaction at high energy is by means of neutrinos. In 1977, when we can hope to begin this work at the SPS, the NAL counter experiments will have operated for four years, and we must expect that the dominant features at the available energies will be known. We expect that useful work can be done at CERN in the way of more precise measurements and more sensitive searches. To this end we should have the best possible neutrino beams and we should also prepare the best possible detectors. Furthermore, they should be ready when the SPS is ready.

2. PHYSICS

In neutrino experiments, present counter techniques are particularly suitable to the identification and measurement of the muons which are produced and to the measurement of the total energy in the hadronic shower. In particular, magnetized iron is very nice, because it combines in itself the properties of a cheap, massive target, hadronic filter, and momentum analyser. The possible experiments then fall into three classes:

i) search for "strange" muons, that is muons of the "wrong" sign (heavy leptons) and multiple muons (tridents, intermediate vector bosons);

ii) study of the inclusive processes

$$\nu(\bar{\nu}) + A \rightarrow A^{*} + \mu^{-}(\mu^{+}) \ ;$$

iii) search for events without muons (neutral currents)

$$\nu(\bar{\nu}) + A \rightarrow A^{*} + \nu(\bar{\nu}) \ .$$

The inclusive processes of type (ii) can be studied as a function of neutrino energy, of momentum transfer and inelasticity, for different nuclei and for ν and $\bar{\nu}$. Corresponding quantities can be studied for processes of type (iii) if neutral hadronic currents contribute a sizeable fraction ($\gtrsim$ 10%) of the total neutrino cross-section.

3. NEUTRINO BEAM

We believe that it is best for counter experiments to concentrate on higher energy. Wide-band neutrino beams have a large excess of

low-energy neutrinos which interfere with the detection of the high-energy events, and it seems best to start with neutrino beams in which the momentum of the primary charged beam is selected. Excellent, and essentially equal, beams of this type have been designed for both North and West areas[1]. Some of the properties of the beam designed by Petrucci for the West Area are given in the Appendix. It has a momentum bite of up to ± 10% and solid angle of $\sim 19 \times 10^{-6}$ sterad, angular divergence of $\sim$ 0.2 mrad and can accept particles up to 275 GeV/c. The background of neutrinos not from the decay region of the beam can be kept to a level of $\sim$ 1%. The dominant neutrinos are from the decay $K \to \mu\nu$ and $\pi \to \mu\nu$. The kaon neutrinos are distributed in momentum uniformly from 0 to 0.96 and the pion neutrinos from 0 to 0.43 of the charged beam momentum. The intensities of kaon and pion neutrinos are shown in Fig. 1. At 275 GeV/c parent momentum they are roughly equal. The more interesting, because of their energy, are the kaon neutrinos. The correlation of neutrino production angle and its momentum is shown in Fig. 2 for a primary energy of 275 GeV/c. If the detector is large enough to detect efficiently neutrinos produced up to $\sim$ 2mrad, the entire neutrino energy spectrum is covered in a single exposure. Kaon neutrinos cover the interval 120-260 GeV/c uniformly, and pion neutrinos the interval 0-120 GeV/c with about twice the intensity (see Fig. 3). The fact that the entire neutrino spectrum is covered in one exposure is experimentally very important, since it obviates the external monitoring of the apparatus, which is difficult and subject to substantial error.

It is important to note that although the entire neutrino spectrum is covered, the energy of the neutrino responsible for a particular event can be known, to the extent to which the neutrino angle is known, and up to a possible ambiguity of whether it is pion or kaon neutrino, and a background of the order of $\sim$ 3% due to K three-body decay. The accuracy of E_ν depends chiefly on the angular divergence of the charged particle beam, its energy definition and the length of the decay path. For the narrow band beams of the Appendix ($\Delta\theta \sim \pm 0.2$ mrad, $\Delta p/p \sim \pm 8.5\%$, decay length 400 m), the resolution in E_ν is approximately ±15%. If the same beam is reduced in angular divergence, in momentum acceptance, and in decay length so that 85% of the beam is sacrificed, the resolution in E_ν can be improved to ±5% (see Fig. 2). We will come back to this point later.

4. MUON DETECTORS

4.1 General

We propose a muon detector which is modular so that it can serve in sections as analyser, or in its entirety as combined target and muon analyser. The length of magnetized iron necessary to achieve 10% muon momentum resolution, in the competition between multiple scattering and magnetic deflection is $\sim$ 4 m, independent of momentum. We consider this a valid length for analyses. At appropriate intervals the trajectory has to be measured and for this purpose we propose drift chambers.

4.2 Iron modules

Diameter. The diameter reflects considerations of cost, neutrino beam diameter, and the divergence of the muon before it has traversed 4 m of iron. For an average distance of 700 m between decay point and detector, and for the 2 mrad acceptance discussed in Section 3, the interactions are contained in a radius of 1.4 m. The angular divergence of the muons is a function of the centre-of-mass emission angle, c.m. inelasticity and neutrino energy. The angle is largest for zero inelasticity in the c.m. In that case (see Fig. 4)

$$\theta_\mu^{lab} = \tan^{-1}\left[\sqrt{\frac{2m_p}{E_\nu}}\sin\theta_{cm}\Big/(1+\cos\theta_{cm})\right] .$$

Because of the large angles at small energies, the muon detector will be geometrically inefficient for small E_ν. The experiment will therefore be poor for $E_\nu \lesssim 30$ GeV. If we focus on a neutrino energy of 100 GeV, most muons have less than 0.2 rad angles, and a reasonable compromise between acceptance and cost might be achieved for a muon detector of $\sim \sqrt{(1.4)^2 + (6 \times 0.2)^2} = 1.85$ m radius or 3.7 m diameter. A sketch of such a module is shown in Fig. 5. The module, 3.75 m diameter and 75 cm of iron in thickness, has been split into five pieces to permit the insertion of a scintillator for rough hadron shower measurement. It is planned to equip initially only a part of the modules with scintillators. Iron weight per module is 66 tons. The coil weight is negligible, the power requirement is 10 kW per module. The cost of each module is estimated between 0.1 and 0.15 MSF. It is proposed to construct 24 such modules. They can be used as a single target-detector unit, or in groups of 6-8 modules as muon detectors for separate targets.

4.3 Drift chambers

One chamber is needed per magnet unit. Each chamber is to be equipped with 3 wire planes at 60° to each other. The sense wire spacing should be ∿ 6 cm. Chambers of the dimensions needed here (3.75 m diameter) have been successfully constructed at Harvard University[2]. The space resolution of these chambers should be ∿ 1 mm, which is sufficient. The drift time is of the order of 1 μsec. The cost will depend on the construction methods which can be developed, but one can hope that it will not be more than 0.025 MSF/chamber for construction, and an equal amount for the electronics for the 200 wires.

5. HADRONIC SHOWER DETECTOR

The hadronic shower detector should have adequate energy resolution (∿ 5% at 50 GeV/c would seem reasonable), be stable and calibrate in pulse height, have a high density, be susceptible of modular construction and be cheap. No glorious, sure-fire solution is known. We feel that the best bet at the moment is a sandwich of iron and plastic scintillator in the 60° geometry used by Prokoshkin in Serpukhov for γ-ray detection. We propose to construct a prototype module which, if successful, would be repeated 11 times for a final detector of 12 modules. Each module consists of 12 iron plates, 3 cm thick and 3 m in diameter. The 1 cm space between plates is occupied by 0.5 cm thick plastic scintillator, in strips 30 cm wide, split on a diameter (see Fig. 6). The 12 scintillator planes of a module are grouped into three interleaved groups of four, each oriented at 60° to each other. Corresponding scintillators of a group of four share the same phototube, so that there are 60 phototubes per module. The two phototubes corresponding to the same strip are combined in their own output so that we end up with 30 pulse-height channels for the 3 × 10 strips. The length of a module is 48 cm, the average density is 6.1 g/cm^3. Each module weighs ∿ 22 tons and will probably cost ∿ 0.2 MSF. A depth of four modules is required to contain the hadronic shower adequately. The 12 proposed modules could be used either as a single target and hadronic detector, or as three separate hadronic detectors to serve three independent targets, such as H_2 and D_2.

6. ELECTRONICS

The requirements on drift-chamber amplifier and read-out electronics are largely determined by the time and space resolution desired. As high counting rates are not expected, a gas with moderate electron drift velocity can be chosen, e.g. C_2H_4 with 5 cm/μsec. For 1 mm r.m.s. space resolution a time digitizer employing a 50 MHz clock frequency is sufficient. Consequently a design based on MECL II integrated circuits should easily provide the desired space resolution.

For each wire a separate fast electronic channel is required comprising amplifier, pulse shaper, cabling to a central electronics station, etc. In fact the largest fraction of the total cost is spent for the electronics necessary for each individual channel. The cost is estimated to be 85 SF per channel, including power and other overheads.

Several individual wire channels can share a set of scalers (or a single scaler and an associated fast memory buffer for several hits) for the time measurement. The additional cost for the time digitizer, wire address generation and buffer store are estimated to be 45 SF per wire. The total cost of 130 SF per wire corresponds to 25 KSF per 3-chamber module.

The electronics would allow the recording of one event in approximately 1 μsec. Although it may take 50-100 μsec to read the event into a computer, no additional dead-time is introduced if sufficient intermediate buffering is provided. It is therefore easily possible to take several events in a burst of 100 μsec spill time.

7. EXPERIMENTAL ARRANGEMENTS

7.1 Possible layout

The modular construction of the iron core magnets and the shower detectors allows different experimental arrangements. Two possibilities are sketched in Fig. 7. In the first, the total hadronic shower detector precedes the total muon detector. Both the hadronic shower part and the magnetized iron part act as target. In the second, the hadron and muon detectors are divided to measure secondaries from interactions in separate targets.

In the first set-up the events originating in the hadronic shower detector are used chiefly in an inclusive study of the q^2-ν plot for charged and neutral currents. Here we may make a comparison with Gargamelle. Our arrangement has the severe disadvantage that all the exclusive features of the process are missed. The advantages are:

- the hadronic energy is measured more easily;
- the muon is identified more clearly; and
- the rates are $\sim$ 20 times higher.

The events originating in the muon detector can be used to search for heavy leptons, intermediate bosons and neutral currents, as well as to study the diagonal process $\nu_\mu + Fe \rightarrow Fe + \nu_\mu + \mu^+ + \mu^-$. Because of its large mass, the rates in this part of the detector will be $\sim$ 200 times higher than those in Gargamelle. The misidentification of muons due to π-μ decays is reduced due to the higher density.

In the first arrangement the hadronic shower detector and the muon detector complement each other quite nicely. The events originating in the high-density shower detector are measured with good accuracy. Furthermore, the large mass and the uniform muon detection efficiency of the muon detector, if used as a target, makes it particularly suited to search for rare events and to measure the inelastic form factors up to the largest momentum transfers where propagator effects from a high-mass intermediate vector boson may become observable.

The second arrangement is restricted to the inclusive study of the q^2-ν plot in H_2 and D_2. With respect to the corresponding experiments in BEBC, the disadvantage is again in the inclusivity of the proposed measurement. The advantages are:

- the neutral component of the hadronic shower is measured;
- the rates are $\sim$ 3 times higher; and
- the muon identification is better;
- the relative normalization between H_2 and D_2 data is naturally given.

7.2 Location of the experiment

Boundary conditions on scheduling in the West Hall and North Hall have been described in the report of the Working Group on neutrino beams for counter experiments[1]. It is clear that all kinds of neutrino beams at present foreseen by counter experiments are possible in the West Area. The neutrino program of BEBC is such that the existence of a perfect iron shielding can be assumed. Furthermore, the running conditions of narrow-band beam bubble chamber and counter experiments are completely compatible. We propose therefore to install this experiment in the West Area.

The total length of the experimental set-up is $\sim$ 40 m. It seems possible to install the experiment in front of BEBC. Considering the neutrino flux, this is in principle the most favourable position; however the available space is tight. Constraints from the RF beam and the general West Area shielding are still being examined. In case there are too many practical difficulties, we would like to install the experiment immediately after BEBC.

7.3 Running conditions

The experiment can be triggered both by a minimum hadron energy deposited in the calorimeter and by a minimum muon track length; for instance, five hits in a row of plastic scintillators placed every meter in the iron core magnet. This corresponds to a cut-off in μ momentum of 5 GeV. One has to consider two sources of background in this trigger:

- Cosmic-ray triggers, estimated to $\lesssim$ 500 per sec.
- Muons from neutrino interactions occurring outside the detector (i.e. in the shield). The number of these triggers is expected to be no more than the number of "good" triggers, since the detector is long compared to the average muon mean-free path.

We expect the order of one event in a narrow-band beam per burst. The drift chamber and read-out dead-time is 1-2 μsec per event. With the "high acceptance" narrow band beam, the presently foreseen 25 μsec spill will be adequate, since even in this short spill the dead-time losses should not be more than 25%. An ideal spill time might be 100-200 μsec, and 1 msec is tolerable. For the same reasons these conditions are optimum for the bubble chamber. We expect that the bulk of the running will be with these conditions.

It may be of interest to take some data with the "tight" narrow band beam, which gives the possibility of good energy resolution on the incident neutrino. This will offer an independent check on the q^2-ν plot measurement. The intensity of this beam is, however, too low to be useful for bubble chamber work, and therefore the amount of running in this beam will be limited.

The wide band, which is considered for BEBC filled with H_2 and D_2, is of limited interest to us, namely only for running with H_2 and D_2 targets, and to some extent for setting up and checking. For the study of neutrino interactions in the iron, the event rate will be too high, the average energy too low, and the spectrum too uncertain. It may very well turn out that this beam will also give difficulties to the BEBC and Gargamelle EMI's and that it will be possible to run this beam only at reduced intensity. In that case, a "high intensity", high-band beam may also be preferred by the BEBC H_2 and D_2 users.

8. GEOMETRICAL ACCEPTANCE AND EXPERIMENTAL RESOLUTION

8.1 Acceptance

The geometrical acceptance of the detector for the inclusive process $\nu + Fe \rightarrow \mu^- + X$ has been calculated for a charged beam energy of 275 GeV. In Fig. 8 the results are shown as a function of E_ν after integration over the q^2-ν plot. For this calculation the density was assumed to be flat in $y = \nu/E_\nu$ and proportional to $(1 - x)$ where $x = q^2/2M\nu$ (spin-$\frac{1}{2}$ parton model).

A minimum track length of the muon of 5 m inside the muon detector was required. The acceptance is shown both for events originating in the hadron shower detector and for events originating in the muon spectrometer. Figure 9 shows the differential acceptance in the x-y plot for three representative energy intervals. In conclusion, the acceptance is satisfactory for both experimental arrangements and nearly all kinematic configurations.

8.2 Resolution

Given the resolution of the drift chambers ($\sim$ 1 mm) the errors on the muon track measurement are dominated by the multiple scattering in the iron core magnets for momenta up to 150 GeV/c. To calculate the invariants

of q^2 and ν, one has also to measure the hadron energy inside the calorimeter (case a) or the neutrino energy from the radial position of the interaction point inside the target in a "tight" beam (case b).

The expected measurement errors in the q^2-ν plot are shown in Fig. 10a and 10b for E_ν = 200 GeV where a hadron energy resolution of $\Delta E_h/E_h = \pm 5\%$ at 200 GeV, ±15% at 20 GeV has been assumed for the calorimeter (a) and $\Delta E_\nu/E_\nu = \pm 5\%$ for the tight beam (b).

The resolution is clearly better for events measured in the calorimeter, useful information can however be deduced also from the events produced inside the iron core magnets. For the latter we have the additional complication that there is an ambiguity in the neutrino energy, since it is not known if the event is coming from a π^- or K-neutrino (hatched region). This ambiguity can be resolved by a coarse hadron energy measurement, inserting scintillators between the iron modules as mentioned before.

If neutral hadronic current events exist, the invariants q^2 and ν can be determined from the neutrino energy and the direction and energy of the hadron shower. The hadron energy is measured in the calorimeter as for muonic events. A crude average hadron direction can be deduced from the shower measurement due to the segmentation of the scintillators with a resolution of approximately 100 mrad. Correspondingly only the inelasticity ν is determined well, whereas the momentum transfer q^2 is measured with large errors.

8.3 Rates

The rate estimates are based on measurements of π^+ and K^+ production on beryllium at 24 GeV [3], scaled to 400 GeV proton energy. Production rates calculated according to different versions of the thermodynamical model[4] are typically of a factor of 2 more favourable. The following table gives event rates at two different settings of the parent beam energy and in the two parts of the detector.

Depending on the actual proton beam intensity available, event rates of the order of 0.2 to 5 per accelerator cycle are expected.

Table 1

Event rates per 10^{12} interacting protons for a nominal narrow band beam energy E_0 ($\Delta p/p = \pm 8.5\%$, 400 m decay, E_p = 400 GeV)

	Events produced in hadron shower detector		Events produced in muon spectrometer	
	E_0 = 200	E_0 = 275	E_0 = 200	E_0 = 275
$E_\nu > E_0/2$	0.10	0.042	0.36	0.16
$E_\nu < E_0/2$	0.10	0.022	0.38	0.08
Total	0.20	0.064	0.74	0.24

9. SUMMARY

It is proposed to set up a counter neutrino experiment with the intention to study neutrino interactions at very high energies. In designing the experiment, particular emphasis has been laid upon neutrino energies in the 100-260 GeV range. A massive target and a detector totalling 1850 tons are combined to overcome the unfavourable rate conditions.

The detector consists in total of 24 modules of iron core magnets and 12 modules of hadronic shower detectors. The detector is well suited for most things which are of interest at the moment. Especially the iron core magnets provide excellent muon detection with smooth and almost full geometrical acceptance. The modular construction permits a certain flexibility in the experimental arrangement. Considering that the status of neutrino physics three years from now is uncertain, this flexibility may turn out to be important.

The desire to start the experiment as early as possible is evident. We propose therefore to install the experiment in the West Area, using the same beam facilities as BEBC. A high-energy narrow-band neutrino beam utilizing 400 GeV protons is important because it offers substantial advantage for clean and accurate measurements. Compared to a wide-band

beam, only a modest amount of intensity has to be sacrificed at the high-energy part of the spectrum.

The total construction cost for the detectors described in this document is estimated to be 6-8 MSF. The time required for development and construction is estimated to be 2-3 years. In order to be sure that we are ready at the end of 1976, we are prepared to engage ourselves immediately. An early decision of the SPSC would therefore be very much appreciated.

* * *

REFERENCES

1) Report of the Working Group on Neutrino Beams for Counter Experiments, CERN/SPSC/T73-4 (1973).

2) D.C. Cheng, W.A. Kozanecki, R.L. Piccioni, C. Rubbia, L.R. Sulak, H.J. Weedon and J. Wittaker, Very large proportional drift chambers with high spatial and time resolution, Harvard University preprint, submitted to the Int. Conf. on Instrumentation for High-Energy Physics, Frascati (1973).

3) D. Haidt, CERN Internal Report TCL 71-111 (1971).
D. Haidt, ECFA Working Group ECFA/WG/72-41 (1972).

4) J. Ranft, CERN Library Program W129.

APPENDIX

NARROW-BAND BEAM IN THE WEST AREA

The design of this beam implies the various constraints of the broad-band beam layout and in particular the direction of the decay tunnel and its reduced diameter (Φ = 1.2 m) for most of its length.

The purpose of this design was, besides the usual requirements, to obtain large angles between the proton direction and the decay tunnel direction, wherever the protons interact (production target or beam stopper). These angles are 15 mrad at the production target and 11 mrad at the beam stopper; this last value might, however, be increased by a further 3 or 4 mrad by means of an iron septum magnet acting on the protons after their separation in space from the secondary beam.

The main data of the beam are (Fig. 11):

maximum momentum	275 GeV/c
total length	99 m
maximum horizontal acceptance	±4.8 mrad
maximum vertical acceptance	±1.28 mrad
maximum solid angle acceptance	19 μsterad
maximum momentum bite	±10%
chromatic dispersion at momentum slit	0.34 cm/%
horizontal magnification at momentum slit	5.1
momentum resolution for 3 mm target	4.5%
r.m.s. divergence at beam exit for $\Delta p/p$ = ±8.5%	∿ 0.2 mrad

The divergence of the beam can be reduced to 0.12 mrad by collimating the beam, and so reducing its acceptance. This collimation should act both on the transmitted momentum bite and on the angular acceptance.

Beam transport elements required for the secondary beam:

quadrupoles	: 10 cm aperture,	gradient 2500 gauss/cm:	16 m
"	: 12 cm aperture,	gradient 2000 gauss/cm:	10 m
bending magnets:	10 cm gap,	field 1.6 Tesla:	20 m
" "	: 7.5 cm gap,	field 1.6 Tesla:	12 m

Figure captions

Fig. 1 : The neutrino flux per interacting proton for a narrow-band beam as a function of the charged beam momentum ($\Delta p/p = \pm 5\%$, $\Delta\Omega$ = 13 μsr, 200 m decay, 400 GeV proton energy). Neutrinos originating from $\pi \to \mu\nu$ and $K \to \mu\nu$ decays are shown separately.

Fig. 2 : The correlation of neutrino production angle and neutrino energy (left-hand scale) and energy resolution (right-hand scale).

Fig. 3 : Schematic neutrino spectrum for a detector accepting neutrino angles up to 2 mrad.

Fig. 4 : The maximum muon angle as a function of neutrino energy in the laboratory system.

Fig. 5 : Sketch of an iron core magnet module.

Fig. 6 : Sketch of a hadronic shower-detector module

Fig. 7 : Experimental arrangements for the study of ν interactions in iron (top) and hydrogen and deuterium (bottom).

Fig. 8 : Geometrical acceptance for events originating in hadron shower detector (solid line) and in iron core magnets(broken line).

Fig. 9a and 9b : Differential acceptance as a function of $x = q^2/2M\nu$ and $y = \nu/E_\nu$ for different neutrino energy intervals and for events originating in the hadron shower detectors (a) and in the iron core magnets (b).

Fig. 10a and 10b: Expected measurement errors in the q^2-ν plot for events generated in the hadron shower detector (a) and the iron core magnets (b). For (b) a tight beam with ±5% neutrino energy definition has been assumed.

Fig. 11 : Narrow-band beam design for the West Area.

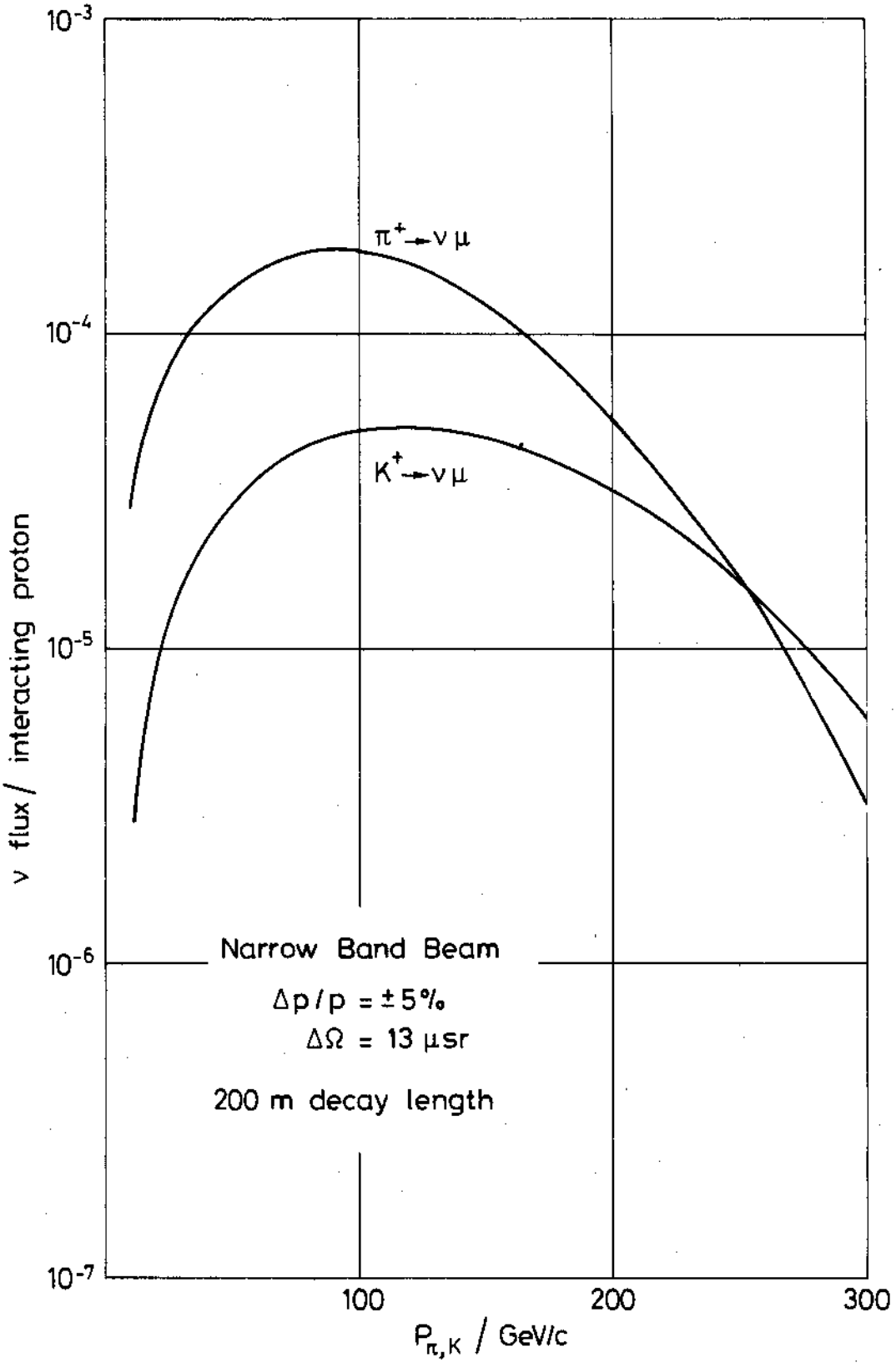
10^{-3}
10^{-4}
10^{-5}
10^{-6}
10^{-7}
$\pi^+ \rightarrow \nu\,\mu$
$K^+ \rightarrow \nu\,\mu$
Narrow Band Beam
$\Delta p/p = \pm 5\%$
$\Delta\Omega$ = 13 μsr
200 m decay length
100
200
300
$P_{\pi,K}$ / GeV/c
ν flux / interacting proton

Fig. 1

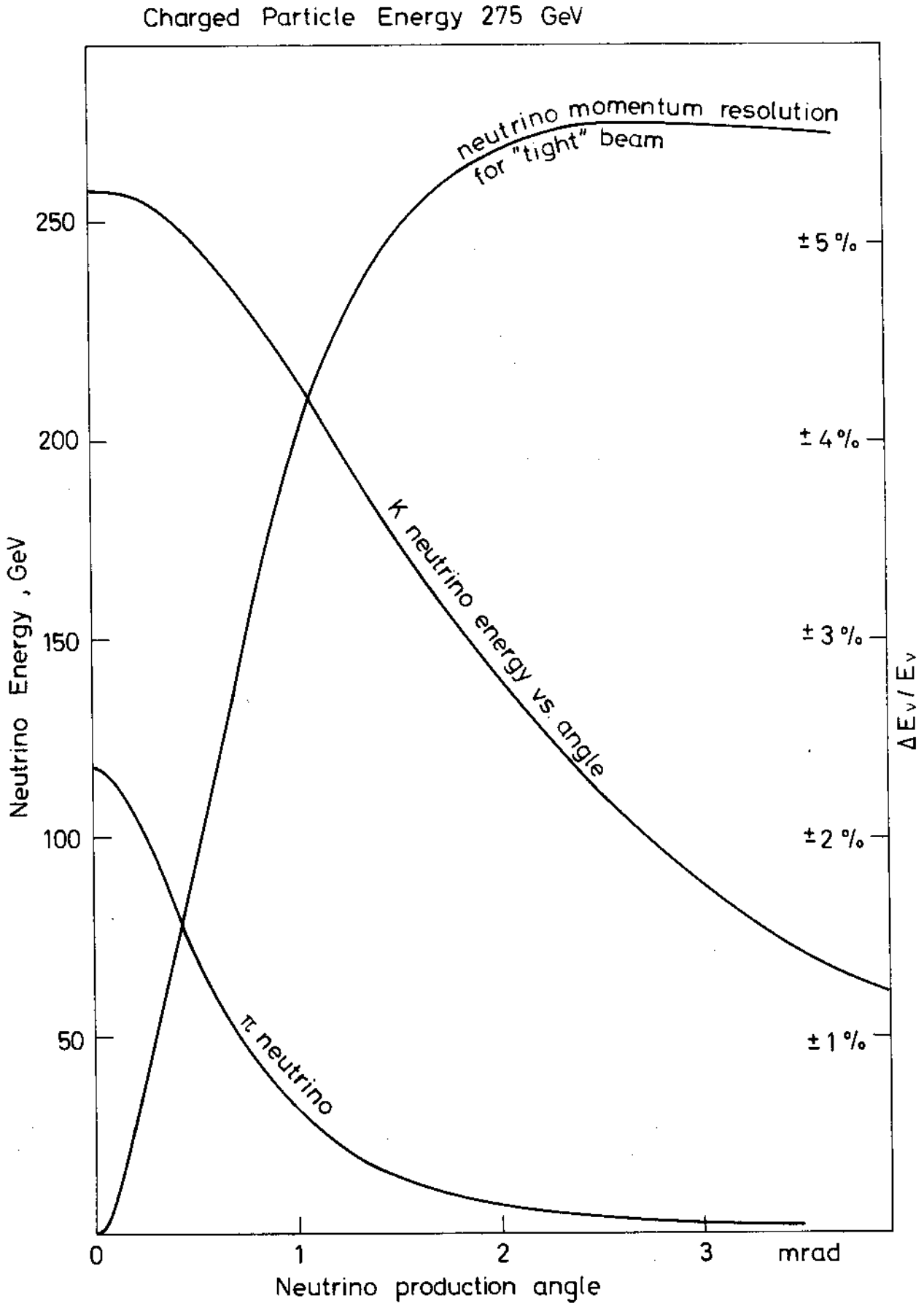
Charged Particle Energy 275 GeV
neutrino momentum resolution
for "tight" beam
K neutrino energy vs. angle
π neutrino
Neutrino Energy , GeV
250
200
150
100
50
± 5 %
± 4 %
± 3 %
± 2 %
± 1 %
ΔEν / Eν
0
1
2
3
mrad
Neutrino production angle

Fig. 2

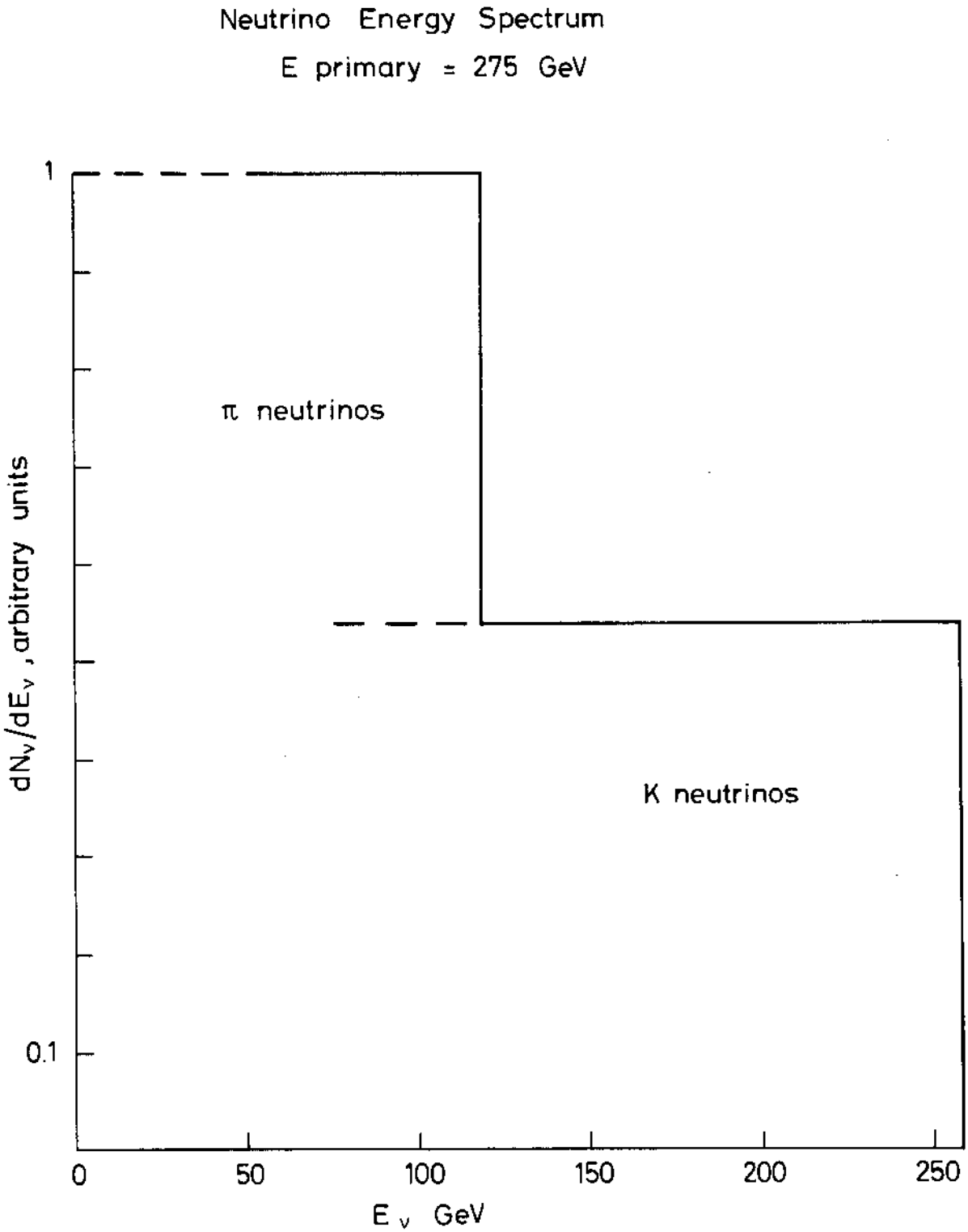
Neutrino Energy Spectrum
E primary = 275 GeV
1
0.1
π neutrinos
K neutrinos
dN_ν/dE_ν , arbitrary units
0
50
100
150
200
250
E_ν GeV

Fig. 3

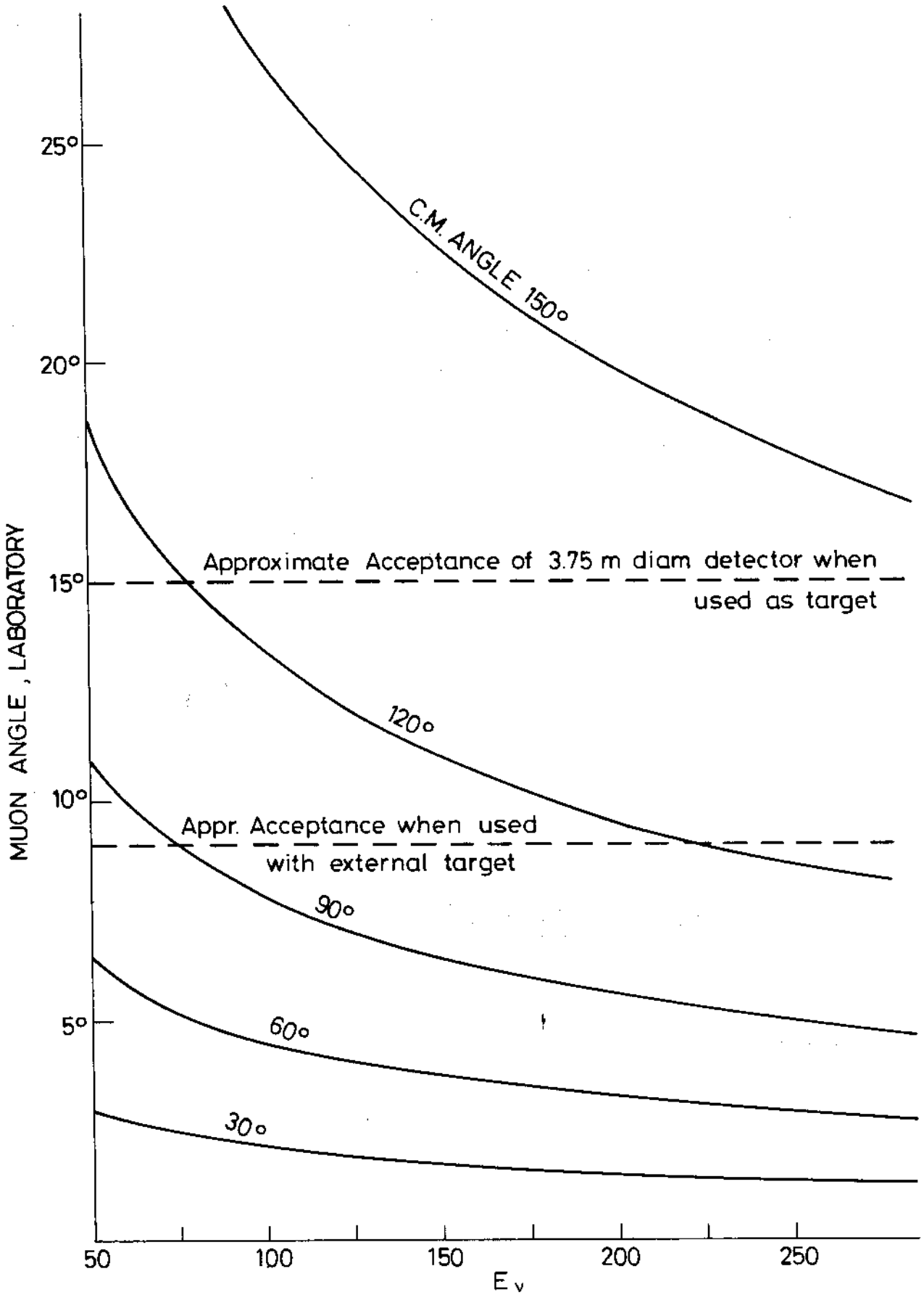
25°
20°
15°
10°
5°
MUON ANGLE , LABORATORY
C.M. ANGLE 150°
Approximate Acceptance of 3.75 m diam detector when used as target
120°
Appr. Acceptance when used with external target
90°
60°
30°
50
100
150
200
250
E ν

Fig. 4

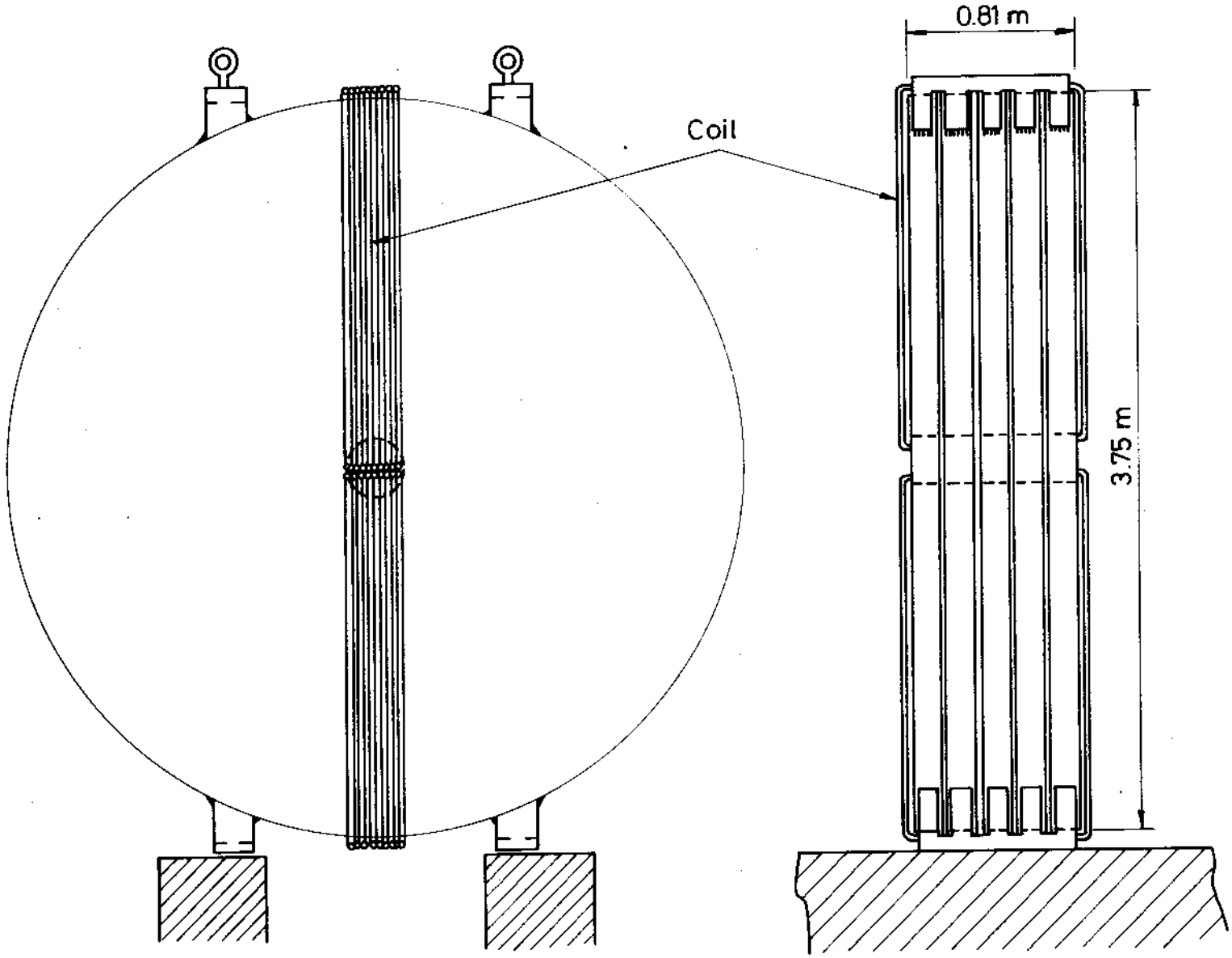

Fig. 5

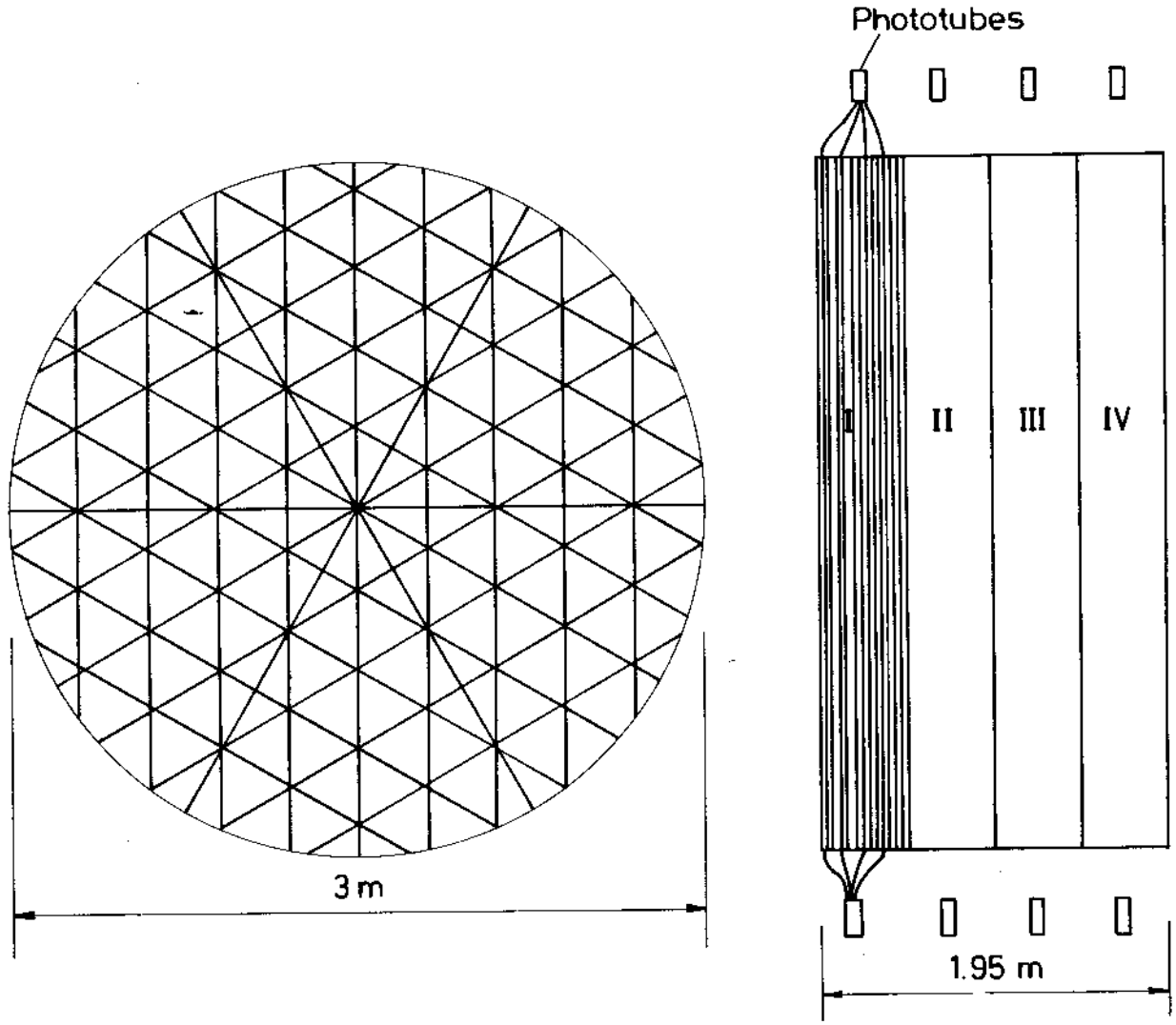

Fig. 6

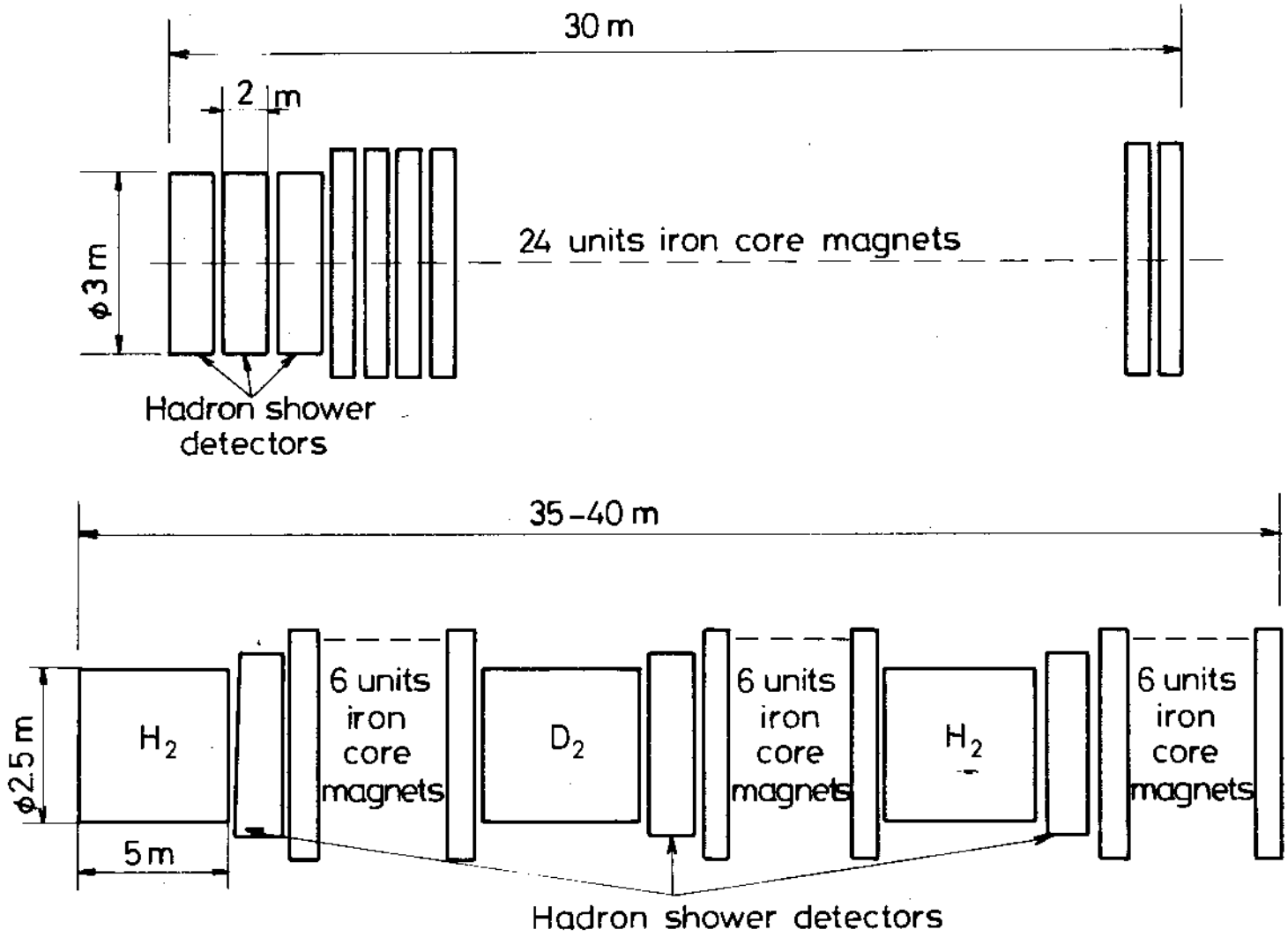
30 m
2 m
φ3 m
24 units iron core magnets
Hadron shower
detectors
35-40 m
φ2.5 m
H2
5 m
6 units
iron
core
magnets
D2
6 units
iron
core
magnets
H2
6 units
iron
core
magnets
Hadron shower detectors

Fig. 7

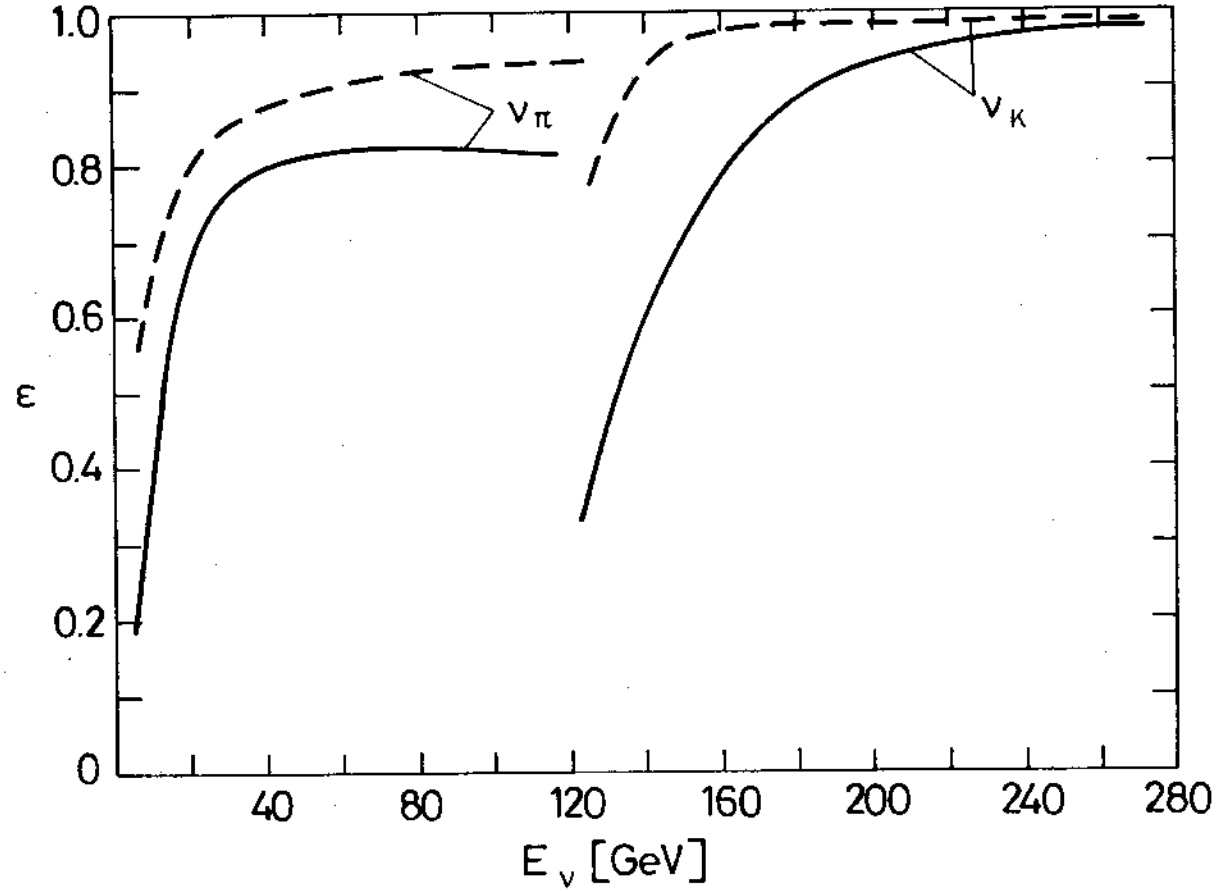

Fig. 8

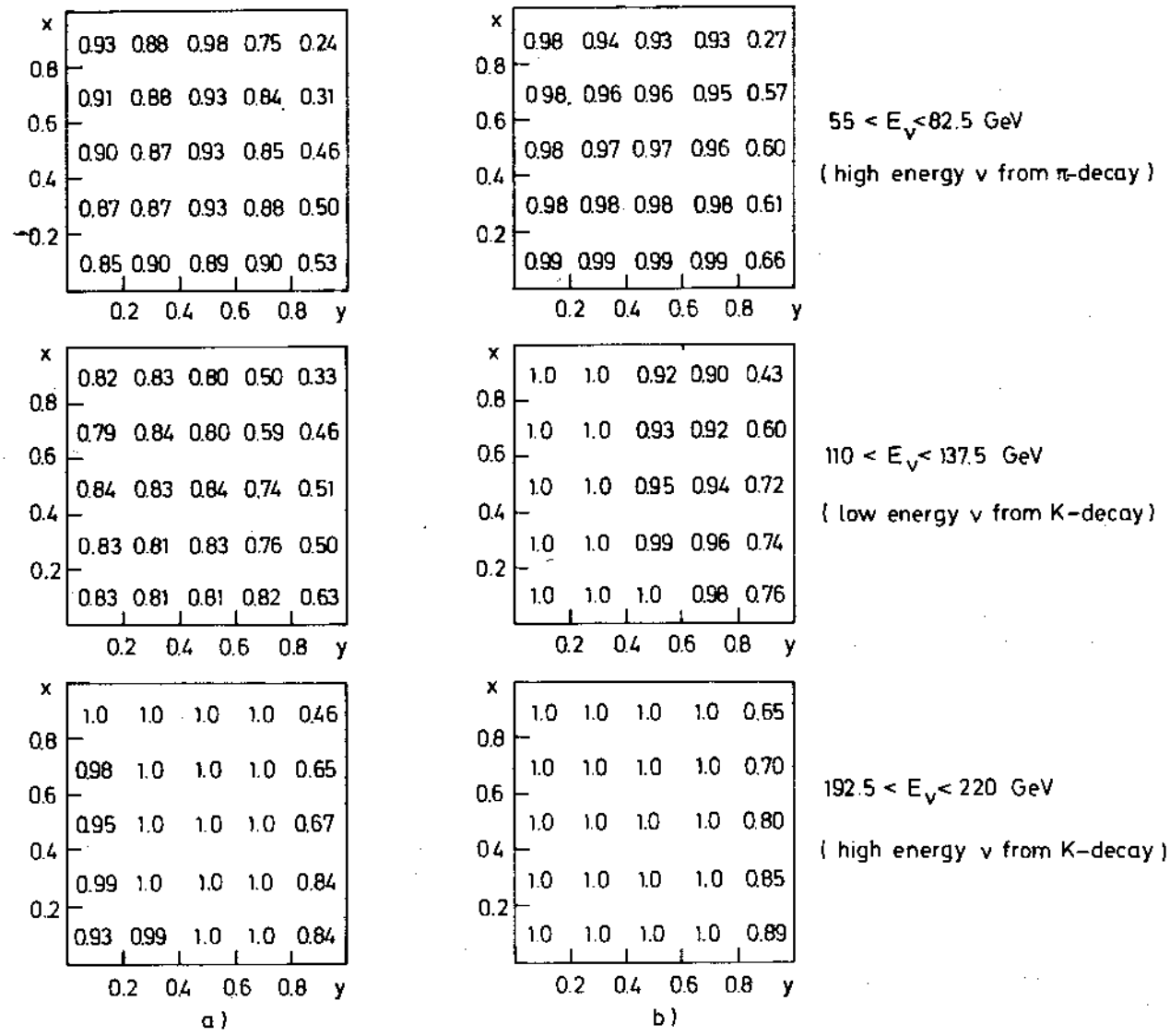

$55 < E_\nu < 82.5$ GeV

(high energy ν from π-decay)

$110 < E_\nu < 137.5$ GeV

(low energy ν from K-decay)

$192.5 < E_\nu < 220$ GeV

(high energy ν from K-decay)

Fig. 9

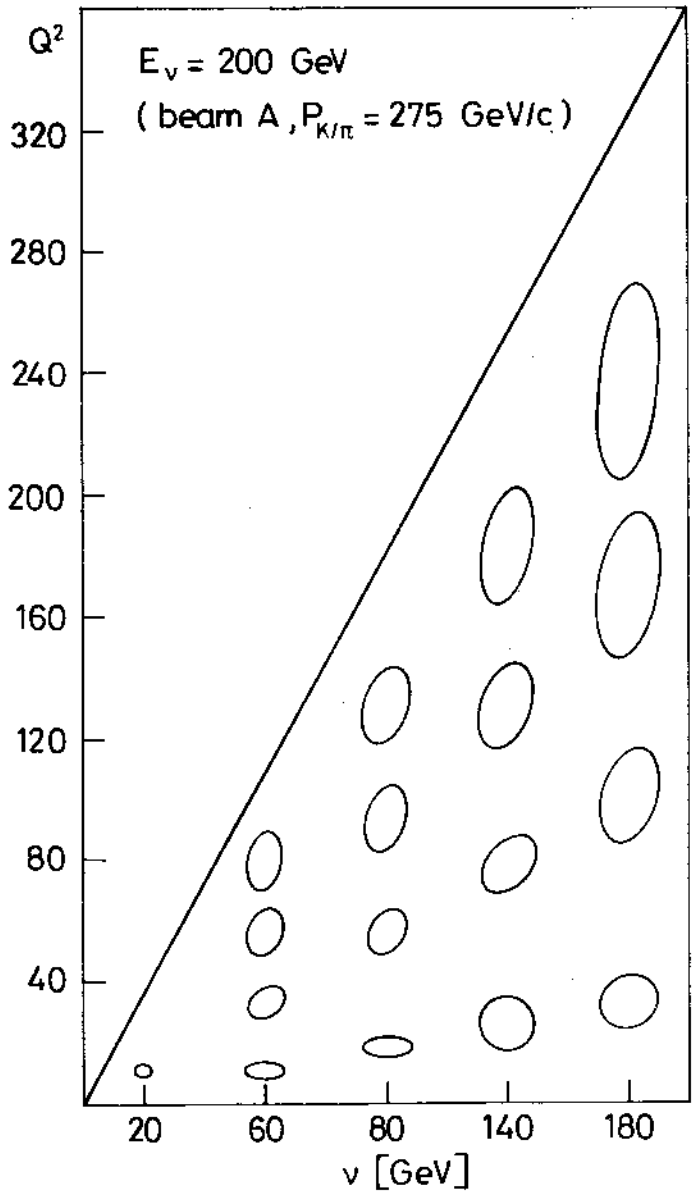
Q^2
E_ν = 200 GeV
(beam A , $P_{K/\pi}$ = 275 GeV/c)
320
280
240
200
160
120
80
40
20
60
80
140
180
ν [GeV]

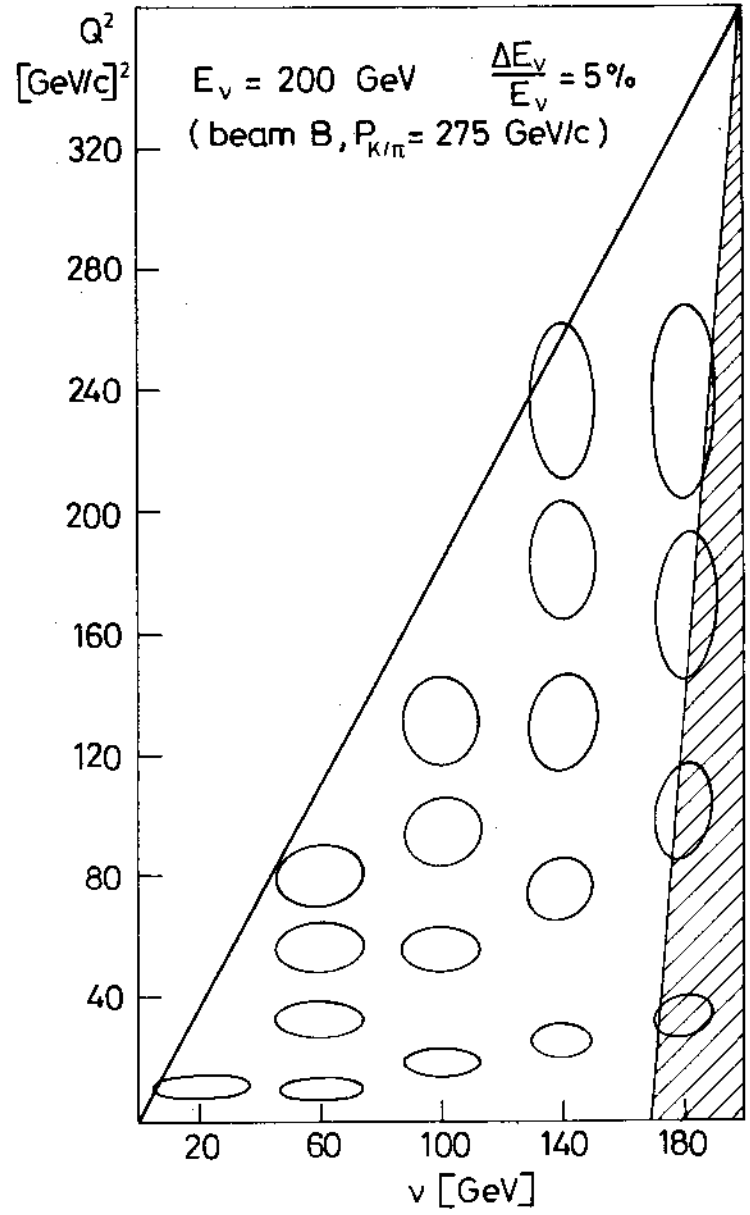
Q^2
$[GeV/c]^2$
E_ν = 200 GeV
$\frac{\Delta E_\nu}{E_\nu}$ = 5%
(beam B , $P_{K/\pi}$ = 275 GeV/c)
320
280
240
200
160
120
80
40
20
60
100
140
180
ν [GeV]

Fig. 10

NARROW BAND NEUTRINO BEAM IN W.A.

Layout with respect to the b.b.v line and optics.

Horizontal profile

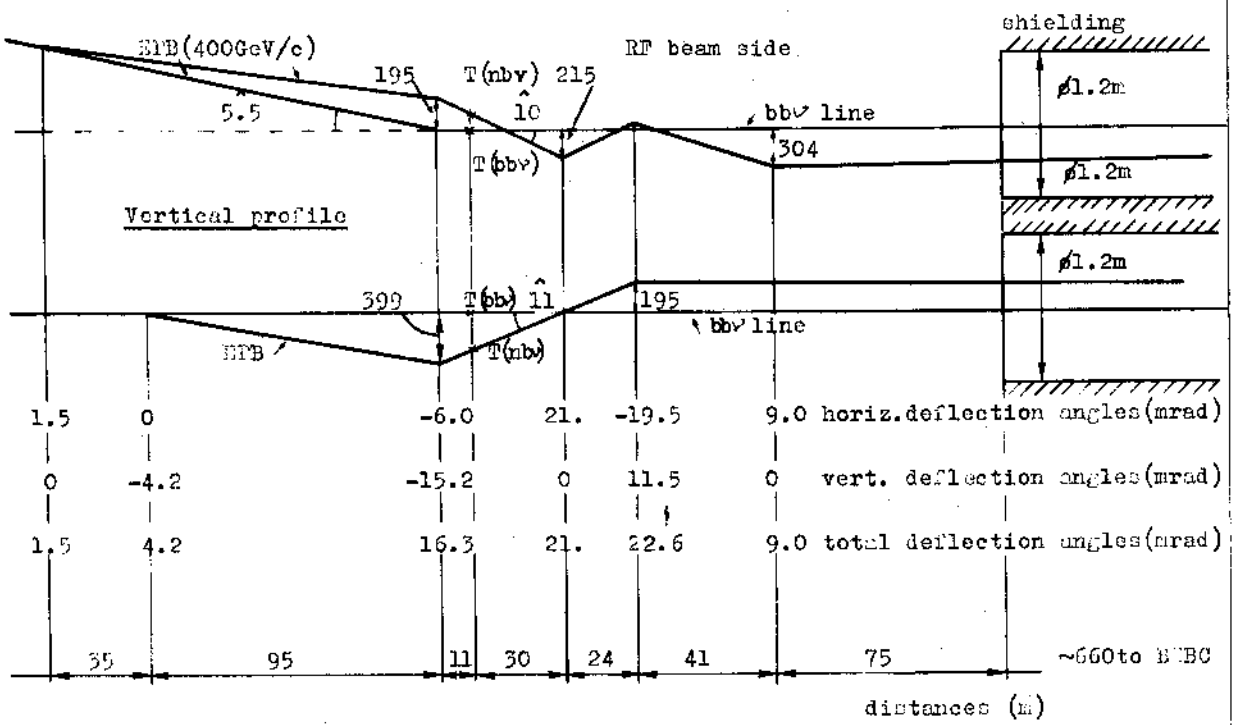

Optics

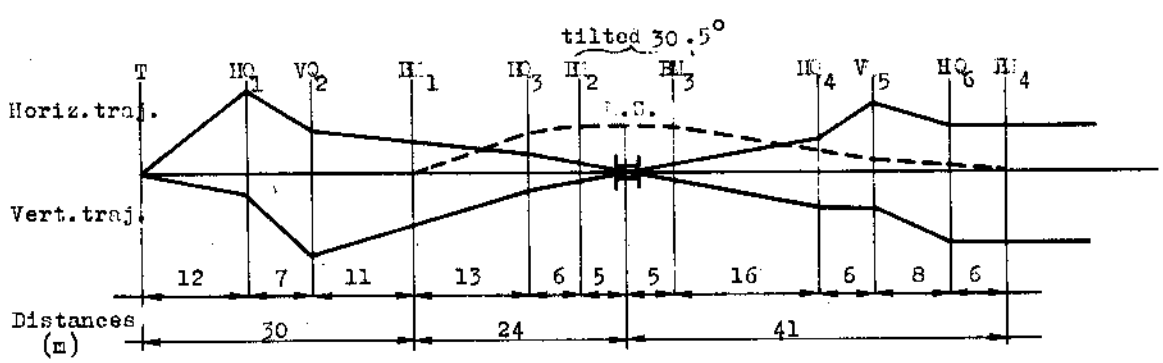

Element length (m)	6	6	12	2	7	7	2	5	3	6	
Aperture or gap (cm)	10	10	10	7.5	10	10	10	12	12	12	7.5
Gradients (gauss/cm) or fields (T)	2520	2485	1.6	1750	1.6	1.6	2000	2060	2000	1.4	

Fig. 11